

Design Guidelines for Spherical Aerostatic Bearings

Dinesh Rakwal, Eberhard Bamberg

University of Utah, Precision Design Lab, Department of Mechanical Engineering, 50 S. Central Campus Dr., Salt Lake City, UT 84112, USA, bamberg@mech.utah.edu

Abstract

This work presents a detailed analytical and experimental analysis of spherical aerostatic bearings with multiple inlets and outlets. Presented are equations for load capacity, stiffness, flow rate, and pressure distribution for the bearings. It uses the Navier-Stokes equations in spherical coordinates while considering the air as a compressible fluid to obtain simple formulas for direct use by the designers. Experiments have been conducted by varying several parameters to validate the theoretical formulas developed for these precision machine elements.

Introduction

Spherical aerostatic bearings are useful in applications involving three rotational degrees of freedom such as satellite motion simulators or a robotic hand joint [1-5]. The main advantage of using these bearings is low stiction (starting friction), low rotational friction and high stiffness. The analytical theory developed for the design of spherical aerostatic bearings is complex and cumbersome to use for design engineers. Existing literature covers equations for design guidelines of aerostatic bearings such as circular, rectangular, cylindrical journal and thrust pad bearings, but little information is available for spherical aerostatic bearings [1-2]. The prediction of the pressure at the inlet of the socket is one of the most crucial and difficult steps in the analytical analysis of any aerostatic bearing [2]. In this work, the equation for the pressure at the inlet of the socket was derived and solved by considering air as a compressible fluid for spherical aerostatic bearing. The equations developed can be used for all types of spherical air bearings including fitted type (socket and ball are of same diameter), clearance type (socket and ball are of different diameter), single inlet and multiple inlets.

Theory

The bearing which was used for the experiments has the geometry as shown in Figure 1. This bearing is a multiple inlets spherical thrust pad bearing. The flow from the inlet is split into two, resulting in an upward (region 1) and downward flow (region 2). If the bearing shown in Figure 1 is displaced downwards, thereby reducing the thickness of the fluid film at the bottom of the bearing, the flow in region 1 is a diverging flow because the sectional area is increasing towards the exit of the flow (outlet at the upper edge of the bearing). The flow in region 2, on the other hand, is converging towards the outlet (bottom of the bearing). The equations were derived for the load capacity, stiffness and flow rate for this type of bearings using the references [1-4].

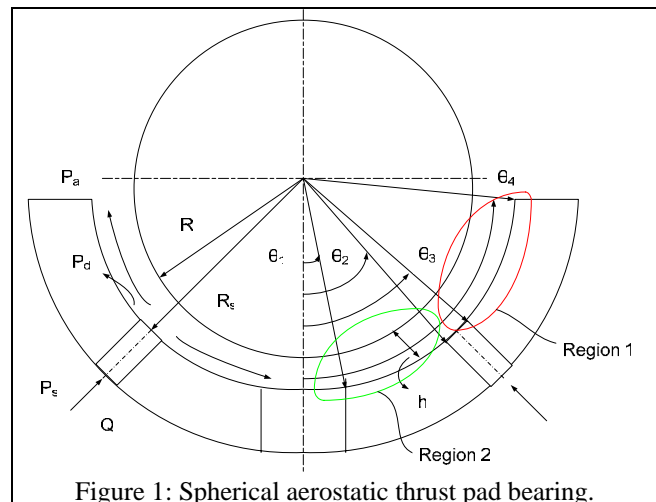


Figure 1: Spherical aerostatic thrust pad bearing.

The total flow rate is [2],

$$Q_d = \frac{p_d^2 - p_a^2}{p_d} \frac{\pi h^3}{12\mu} \left[\frac{1}{\left[\ln \left(\tan \left(\frac{\theta_4}{2} \right) \right) - \ln \left(\tan \left(\frac{\theta_3}{2} \right) \right) \right]} + \frac{1}{\left[\ln \left(\tan \left(\frac{\theta_2}{2} \right) \right) - \ln \left(\tan \left(\frac{\theta_1}{2} \right) \right) \right]} \right]$$

The load capacity of the bearing is [2],

$$W = W_{up} + W_{down}$$

$$W_{up} = \int_{\theta_3}^{\theta_4} \left\{ p_d^2 - (p_d^2 - p_a^2) \frac{\left[\ln \left(\tan \left(\frac{\theta}{2} \right) \right) - \ln \left(\tan \left(\frac{\theta_3}{2} \right) \right) \right]}{\left[\ln \left(\tan \left(\frac{\theta_4}{2} \right) \right) - \ln \left(\tan \left(\frac{\theta_3}{2} \right) \right) \right]} \right\}^{1/2} 2\pi R_B^2 \sin \theta \cos \theta d\theta$$

$$W_{down} = \int_{\theta_1}^{\theta_2} \left\{ p_d^2 + (p_d^2 - p_a^2) \frac{\left[\ln \left(\tan \left(\frac{\theta}{2} \right) \right) - \ln \left(\tan \left(\frac{\theta_2}{2} \right) \right) \right]}{\left[\ln \left(\tan \left(\frac{\theta_2}{2} \right) \right) - \ln \left(\tan \left(\frac{\theta_1}{2} \right) \right) \right]} \right\}^{1/2} 2\pi R_B^2 \sin \theta \cos \theta d\theta$$

The equation for the stiffness of the bearing is similar to equation [3]

$$k = -\frac{dW}{dp_d} \frac{dp_d}{dB} \frac{dB}{dh}$$

The pressure at the inlet of socket as shown in Figure 1 is found as [3]

$$p_d = \sqrt{p_a^2 + p_s B \left[\left(\frac{p_d}{p_s} \right)^{2/\gamma} - \left(\frac{p_d}{p_s} \right)^{\gamma+1/\gamma} \right]}$$

$$\text{Where } B = \frac{12C_d A \mu \sqrt{2RT}}{\pi h^3} \frac{\ln \left(\frac{\tan \frac{\theta_2}{2}}{\tan \frac{\theta_1}{2}} \right) \ln \left(\frac{\tan \frac{\theta_4}{2}}{\tan \frac{\theta_3}{2}} \right)}{\ln \left(\frac{\tan \frac{\theta_2}{2}}{\tan \frac{\theta_1}{2}} \right) + \ln \left(\frac{\tan \frac{\theta_4}{2}}{\tan \frac{\theta_3}{2}} \right)} \sqrt{\frac{\gamma}{\gamma-1}} \text{ and } A = \pi d_o h \text{ [5,6]}$$

The equations above were derived for a constant film thickness h . However, the bearing will be displaced out of the center as soon as a load is applied. In this case, the actual film thickness will be $h_\theta = C(1 + \varepsilon \cos \theta)$ for the top half of the bearing and $h_\theta = C(1 - \varepsilon \cos \theta)$ for the bottom half, respectively. Clearly, the film thickness no longer remains uniform but varies with respect to the angle θ . The above equations become extremely difficult to solve if this varying film thickness is to be considered. Instead, it was found that if the results are multiplied with factor $\frac{\cos \theta_4 + \cos \theta_1}{2}$, the calculated results closely match the actual results obtained from experiments.

Nomenclature

γ Ratio of specific heat of air	h Film thickness	R Gas constant
ε Eccentricity ratio	p Pressure, p_d inlet, p_s supply, p_a atmospheric	R_B Radius of ball
θ Angle measured from load line	e Displacement of ball	T Room temperature
μ Viscosity of air	C Clearance of the bearing	
d_o Diameter of orifice	C_d Discharge coefficient	

Bearing Prototype

The spherical aerostatic bearing is based on a 19.05mm ($3/4''$) size socket diameter. To replicate the spherical bearing surface, a master ball with a diameter that is $12\mu\text{m}$ smaller than the diameter of the bearing sphere was selected [5]. The epoxy used was aluminum filled, low-shrinkage epoxy casting resin (*FMSC 801*, Freeman Supply). Separation of the master surfaces from the replicated surfaces was achieved by applying a thin film of silicon (*Synlube 531*, Freeman Supply) prior to the casting. The orifice diameter for this bearing was chosen to be $400\mu\text{m}$.

Experimental Setup

The spherical aerostatic bearing was tested by displacing the bearing sphere incrementally out of its no load position. After each increment, the applied load was measured using a strain-gage based load cell. The load cell has a range of 0-110N and a resolution of 0.5% of full scale, resulting in load measurements with a resolution of 0.5N.

Results

Results were plotted for the air film thickness at different inlet pressure. The plots for stiffness and load capacity are shown in Figures 4-6 respectively. The plots depict the theoretical values, experimental values and theoretical values with the correction factor.

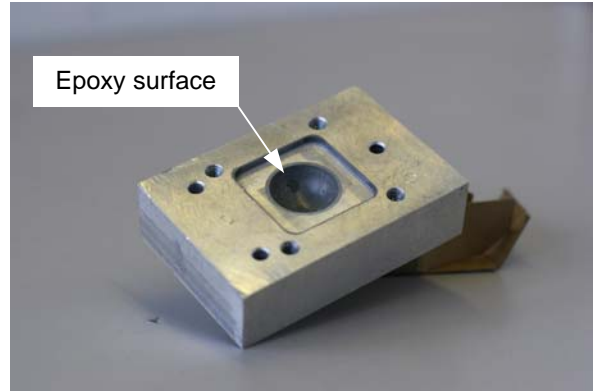


Figure 2: Bearing cavity that was created by replicating the surface using a "master ball" into a thin layer of low-shrinkage epoxy [7].

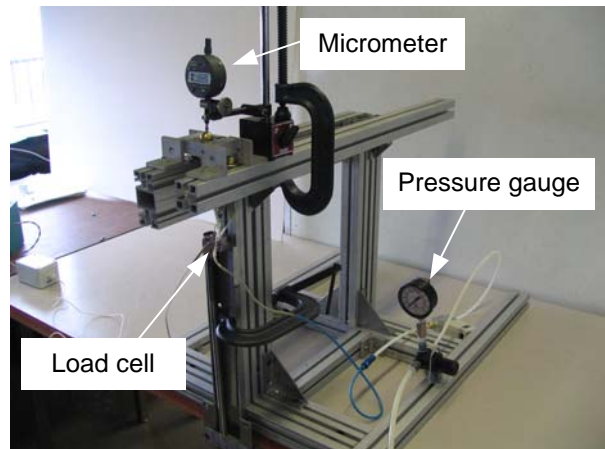


Figure 3: Experimental setup showing the bottom half of the bearing. The bearing is incrementally displaced vertically down while measuring the applied load with a load cell.

Table 1: Comparison between measured and predicted stiffness values

Pressure (bar)	Predicted(N/ μm)	Measured(N/ μm)	Deviation(%)
3	1.5	1.35	10
4	1.9	1.4	26.3
5	2.3	2.1	8.7
6	2.6	2.35	9.6

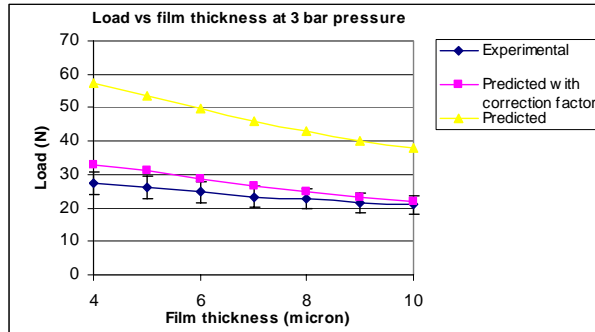


Figure 4: Load vs. film thickness at 3bar pressure.

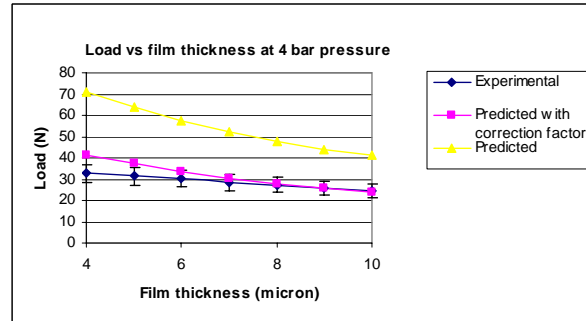


Figure 5: Load vs. film thickness at 5 bar pressure.

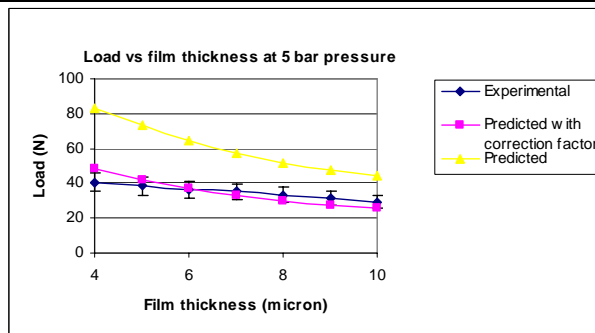


Figure 6: Load vs. film thickness at 5 bar pressure.

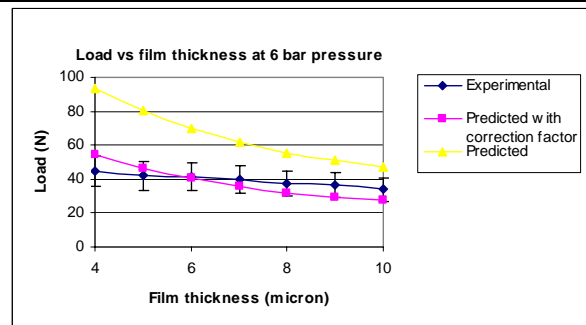


Figure 7: Load vs. film thickness at 6 bar pressure.

Conclusions

Spherical aerostatic bearings are used in spherical joints and other applications which require three degrees of freedom. A new method to predict the bearing performance was developed which allows the pressure at the inlet of the bearing socket to be calculated through numerical methods. An alternative and simpler approach for calculation of load capacity, stiffness and flow rate with error compensation was proposed. Experiments were carried out to verify the theoretical results. In order to reduce the complexity of the calculations involved, a simple correction factor was proposed that allows single and multiple inlet bearings to be analyzed with reasonable accuracy. Further it is shown that the theoretical predictions agreed well with the data obtained from the experiments.

References

- [1] D.F. Wilcock, "Design and performance of gas-pressurized, spherical, space-simulator bearings", *Journal of Basic Engineering*, 1965, 87, pp. 604-12.
- [2] John H. Laub, Robert H. Norton, JR, "Externally pressurized spherical gas bearings", *American Society of Lubrication Engineers transactions*, 1961, 4, pp. 172-80.
- [3] I.C. Tang, W.A. Gross, "Analysis and design of externally pressurized gas bearings", *American Society of Lubrication Engineers transactions*, 1962, 5, pp. 261-84.
- [4] T.L. Corey, C.M. Tyler, JR., H.H. Rowand, JR., E.M. Kipp, "Behavior of air in the hydrostatic lubrication of loaded spherical bearings", *ASME*, 1956, 78, pp. 893-98.
- [5] J.W. Powell, "Design of aerostatic bearings", *The Machinery Publishing Co.*, 1970.
- [6] Alexander H. Slocum, "Precision Machine Design", *Society of Manufacturing Engineers*, 1994.
- [7] Alec Robertson, "Design and calibration of high accuracy spherical joints", *Master's thesis, MIT*, 2003.